Dieses Dokument ist eine Zweitveröffentlichung (Postprint) /

This is a self-archiving document (accepted version):

D. Pohla, V. V. Solovyev, S. Röher, Gärtner, I. V. Kukushkin, T. Mikolajicka, A. Großer, S. Schmult

Carbon-doped MBE GaN: Spectroscopic insights

Erstveröffentlichung in / First published in:

Journal of Crystal Growth. 2019, 514, S. 29-35 {Zugriff am: 06.09.2022}. Elsevier. ISSN 0022-0248.

DOI: https://doi.org/10.1016/j.jcrysgro.2019.02.041

Diese Version ist verfügbar / This version is available on:

https://nbn-resolving.org/urn:nbn:de:bsz:14-qucosa2-812018

Dieses Werk ist lizenziert unter einer Creative Commons Namensnennung – Nicht kommerziell – Keine Bearbvieitungen 4.0 International Lizenz.
This work is licensed under a Creative Commons Attribution-NonCommercial-NoDerivaties 4.0 International License.

Final edited form was published in "Journal of Crystal Growth". 2019, 514, S. 29-35. ISSN 0022-0248.
https://doi.org/10.1016/j.jcrysgro.2019.02.041

Carbon-doped MBE GaN: Spectroscopic insights

D. Pohl[a,*], V.V. Solovyev[b], S. Röher[a], J. Gärtner[c], I.V. Kukushkin[b], T. Mikolajick[a,c], A. Großer[c], S. Schmult[a]

[a] TU Dresden, Electrical and Computer Engineering, Institute of Semiconductors and Microsystems, Nöthnitzer Str. 64, 01187 Dresden, Germany
[b] Institute of Solid State Physics RAS, 142432 Chernogolovka, Moscow district, Russia
[c] Namlab gGmbH, Nöthnitzer Str. 64, 01187 Dresden, Germany

ABSTRACT

The predicted acceptor impurity nature of carbon in hexagonal GaN grown by molecular-beam epitaxy (MBE) is revisited spectroscopically in the energy range between 1.6 and 3.5 eV. Photoluminescence (PL) spectra from ultra-pure GaN and material doped with carbon at a level of 1·18 cm^{-3} differ significantly in the energy range between 3.0 and 3.3 eV depending on the Ga/N stoichiometry during MBE growth. Acceptor-like features for-merly attributed to carbon, beryllium or magnesium incorporation are found for both, undoped and carbon-doped GaN. The intensity of these features depends on the Ga/N stoichiometry during growth. While for Ga-lean surface regions, exhibiting multiple 10 nm deep pits, the observed PL features are found to be less intense compared to Ga-rich surface regions, the situation reverses for carbon-doped material. For all samples, the intensity of the yellow luminescence band around 2.2 eV is weak. The results point at crystal defects and the unintentionally present oxygen as the origin of the spectroscopic features traditionally attributed to carbon in GaN.

1. Introduction

GaN with its wide band gap of 3.4 eV becomes commercially more and more relevant for high power and light emitting electronic devices. Advanced bipolar schemes require controlled n and p doped layers. While n type material is easily realized by silicon doping, magnesium seems to be the only viable p type dopant for GaN, with its numerous disadvantages such as high thermal ionization energy (120 250 meV [1,2]) and a tendency for self compensation at high doping levels [2]. It is known to migrate towards the surface at high growth temperature [3] and it tends to form defect structures. Additionally a post growth thermal treatment is required to "activate" the Mg acceptors by crowding out passivating hydrogen atoms which saturate Mg bonds [4 6].

P type conductivity with another practical acceptor element was not demonstrated so far in hexagonal GaN with any growth technique. Carbon in GaN has been discussed extensively because of its prevalence as an unintentional impurity (along with hydrogen and oxygen) as well as its potential as an intentional dopant [7]. When substituting nitrogen (C_N), C could, in principle, act as an alternative p type dopant [8], re presenting the shallowest known acceptor in GaN [1]. Within the last decade significant theoretical [8 10] and experimental work has been devoted to investigate the effect of carbon incorporation into the GaN lattice during crystal growth. Carbon doping in HVPE and MOCVD thin film growth has been investigated by several groups [7,11 13], un fortunately ultra pure reference samples with a low impurity back ground were typically not included in a comparison with intentionally doped ones. In contrast, the MBE technique represents a controllable method for carbon incorporation independent of other growth para meters [7] along with a typically low and more controllable residual impurity incorporation. Reports on C doped GaN grown by MBE uti lized different organic carbon sources such as CCL_4 [15 17], CH_4 cracked in plasma [18], CBr_4 [12] or CS_2 [11] as well as graphite evaporated with an electron beam [18]. All wurtzite GaN layers re sulted in semi insulating (SI) [18] or insulating [12] films thus de monstrating the feasibility to compensate residual n type conductivity in high electron mobility transistor (HEMT) structures [12,14 19]. At moderate doping levels (10^{18} cm^{-3}) Armitage et al. [11] found an anomalous carbon incorporation behavior: beneath 10^{18} cm^{-3} C com pensates residual n type conductivity, while at an increased C con centration no p type conductivity appeared accompanied by a dete rioration of electrical and optical properties attributed to C_{Ga} and carbon interstitial (C_i) incorporation instead of C_N. Here, the role of the used carbon precursors and/or activation technique and therefore the

* Corresponding author.
E-mail address: diana.pohl@tu-dresden.de (D. Pohl).

Provided by Sächsische Landesbibliothek - Staats- und Universitätsbibliothek Dresden

Final edited form was published in "Journal of Crystal Growth". 2019, 514, S. 29-35. ISSN 0022-0248.
https://doi.org/10.1016/j.jcrysgro.2019.02.041

Table 1
Overview of the discussed samples including the substrate characteristics and doping levels.

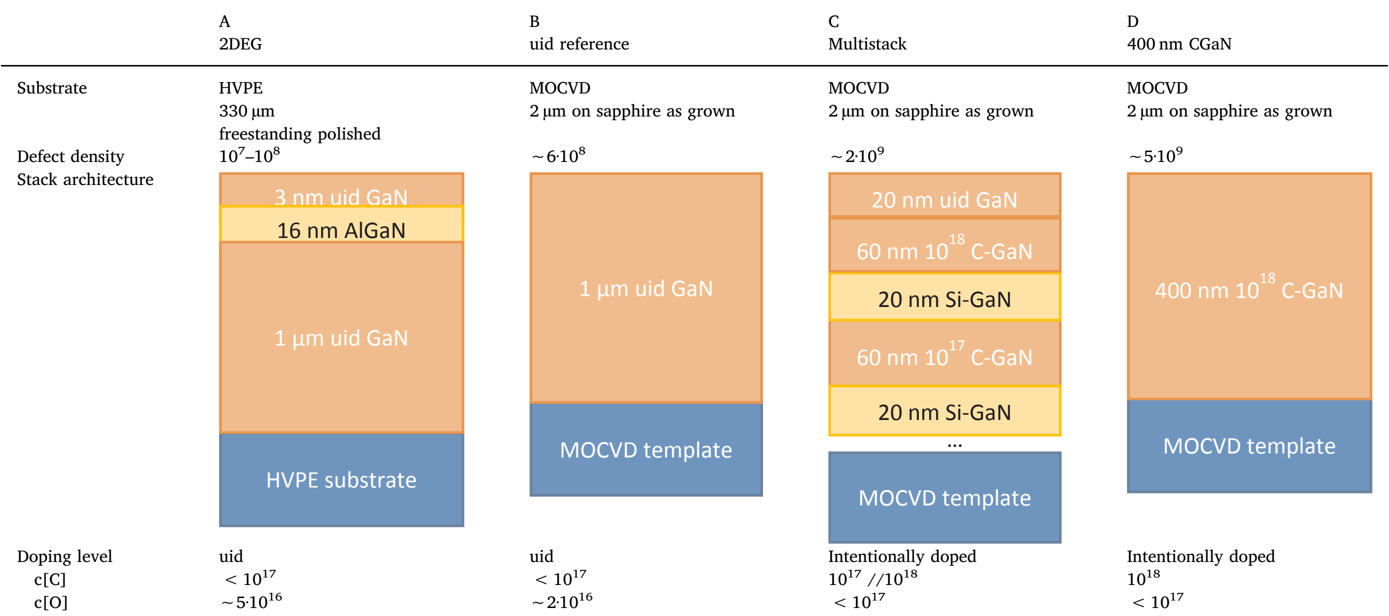

	A 2DEG	B uid reference	C Multistack	D 400 nm CGaN
Substrate	HVPE 330 µm freestanding polished	MOCVD 2 µm on sapphire as grown	MOCVD 2 µm on sapphire as grown	MOCVD 2 µm on sapphire as grown
Defect density	10^7–10^8	~ $6{\cdot}10^8$	~ $2{\cdot}10^9$	~ $5{\cdot}10^9$
Stack architecture	3 nm uid GaN 16 nm AlGaN 1 µm uid GaN HVPE substrate	1 µm uid GaN MOCVD template	20 nm uid GaN 60 nm 10^{18} C-GaN 20 nm Si-GaN 60 nm 10^{17} C-GaN 20 nm Si-GaN ... MOCVD template	400 nm 10^{18} C-GaN MOCVD template
Doping level	uid	uid	Intentionally doped	Intentionally doped
c[C]	< 10^{17}	< 10^{17}	10^{17} //10^{18}	10^{18}
c[O]	~ $5{\cdot}10^{16}$	~ $2{\cdot}10^{16}$	< 10^{17}	< 10^{17}

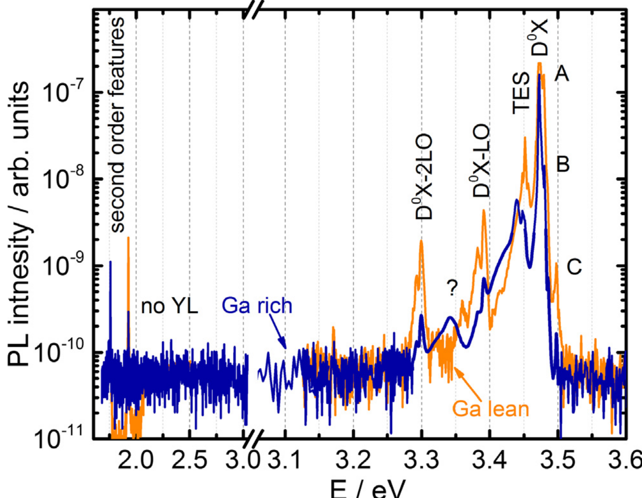

Fig. 1. PL spectra measured at 15 K of sample A representing a clean reference sample from the Ga-lean (orange) and the Ga-rich (blue) region. The samples features an unintentional oxygen background below $1{\cdot}10^{17}$ cm^{-3}, which is the only detectable impurity. Free and donor-bound exciton features D^0X around 3.48 eV are visible in low-temperature photoluminescence combined with a two-electron satellite at 3.43 eV and D^0X-1LO and D^0X-2LO around 3.4 and 3.3 eV. Additionally an unidentified feature at 3.36 eV appears. Around 2.2 eV no yellow luminescence (YL) peak is found. At 1.7 and 1.9 eV the second diffraction order peaks can be assigned to the excitonic feature and the laser line, respectively.

chemical state of the incorporated C atoms (/molecules) is named as root cause of differences in the binding state within the GaN lattice and as result in the electrical and optical properties.

Theoretical calculations and analytical techniques like photoluminescence (PL) found different effects of carbon incorporation into the GaN lattice. C_N was interpreted to become a deep acceptor in one study [20] while calculations in [8,9,21] predicted it to be a shallow acceptor. Contrary, PL data pointed towards C_{Ga} being a shallow donor or forming C_I or C_I C_N complexes [8,9]. Wright et al. [9] stated, that depending on the growth conditions and the Fermi level position at the growth front C doping favors self compensation. Most authors emphasized that the correlation of the C incorporation and the conductivity type is depending on the Ga/N growth stoichiometry. Defects in GaN could act as nitrogen vacancy V_N representing a shallow donor [22] and gallium vacancy V_{Ga} as shallow acceptor, respectively, according to previous calculations [21,23]. In non complexed systems or in complex with other impurities carbon acts as deep acceptor [9,21]. In summary there are competing crystallographic defect mechanisms [7], material properties and often an uncontrollable impurity background in the GaN lattice grown with various techniques that make the analytical identification of the effect of carbon doping challenging.

In this study we focus on the PL analysis of carbon doped MBE GaN layers to address the link between C incorporation and spectroscopic features in the energy region 3.0 3.3 eV and around 2.2 eV (yellow luminescence). Seager et al. [8] reported a broad blue PL band at 3.0 eV instead of the UVL band, which has been observed in semi insulating C doped GaN. They attributed this blue band to transitions from C_{Ga} donor to C_N acceptor. Polyakov et al. [24] also noted an enhancement of the blue band peaked at 3.05 eV in GaN samples heavily contaminated with carbon. Reuter et al. [25] observed a broad red luminescence band with its maximum at 1.64 eV in C doped GaN. Several authors noted a correlation between the YL band intensity and C doping although the properties of the YL band in undoped and C doped GaN were apparently different [26]. There is a controversial discussion about the origin of the yellow luminescence (YL) band between 1.9 and 2.3 eV. Suski et al. [27] pointed out that many theories and discussions of experimental results regarding the yellow emission band are based on a strong electron lattice coupling interaction. Hofmann et al. [28] performed steady state and time resolved PL measurements on unintentionally doped (uid) MOCVD GaN. They found a deep center, but the presence of the YL in almost all kinds of GaN samples independent of the growth techniques indicates the YL is rather of intrinsic origin. The V_N as well as the Gallium interstitial Ga_I were earlier suggested by Glaser et al. [29] to act as intrinsic donors in GaN and therefore might be candidates. Furthermore, on the basis of spatially resolved measurements it was found that the YL intensity greatly increases towards to the interface to the substrate [29]. This finding also indicates that native defects and/or interface contaminations are involved. Their experiments strongly support a shallow donor deep acceptor model for the recombination mechanism of the yellow PL in GaN. This is consistent with our previous observation, that YL weakens with a lower

Provided by Sächsische Landesbibliothek - Staats- und Universitätsbibliothek Dresden

Final edited form was published in "Journal of Crystal Growth". 2019, 514, S. 29-35. ISSN 0022-0248.
https://doi.org/10.1016/j.jcrysgro.2019.02.041

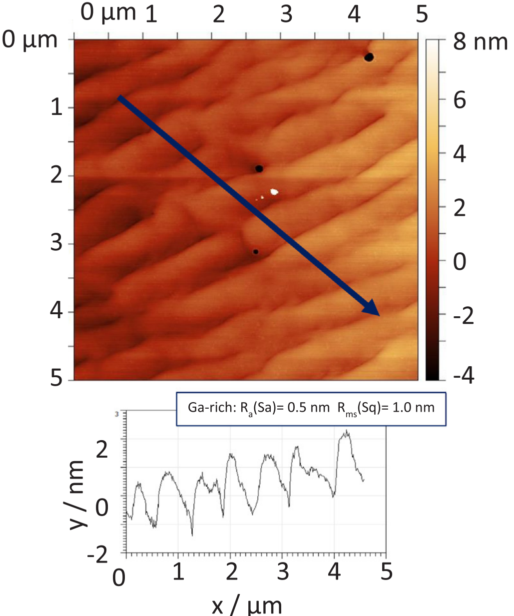

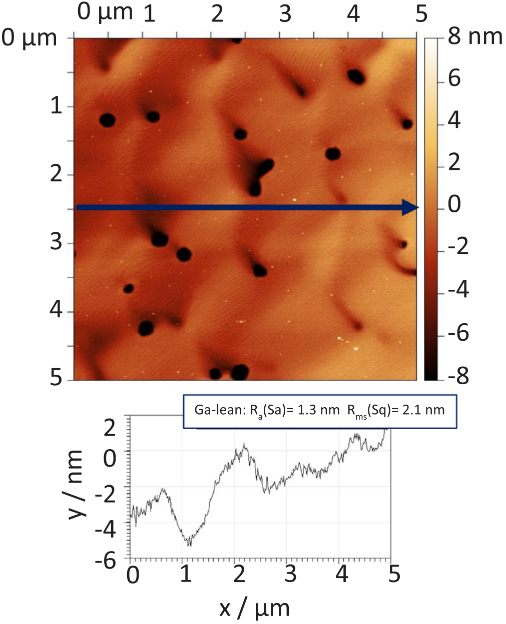

Fig. 2. AFM surface morphology from Ga-rich (left figure) and Ga-lean (right figure) region of sample A showing monolayer steps and terraces for the Ga-rich and monolayer steps with single pits for the Ga-lean part of the sample. The according linescans and the overall surface roughness R_a and R_{ms} are presented below the respective AFM image.

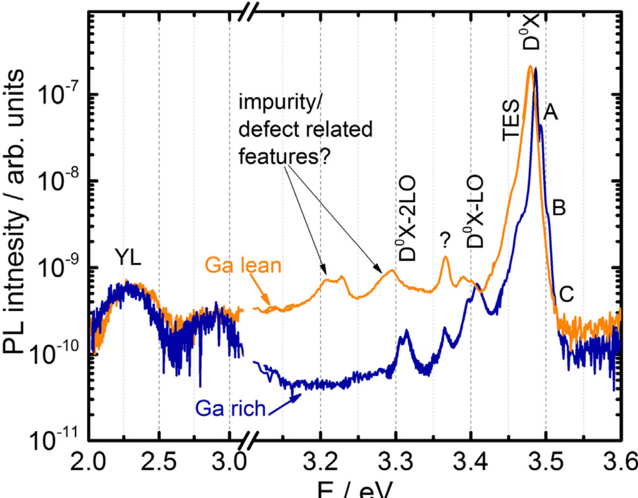

Fig. 3. PL spectra measured at 15 of a 1 µm thick uid GaN layer (sample B) with a carbon and oxygen doping level significantly below 10^{17} cm^{-3} prepared under Ga-lean growth conditions (orange) and prepared under Ga-rich conditions (blue). The PL from Ga-lean region exhibits characteristic 'dopant' features. Yellow luminescence around 2.2 eV, which is often associated with carbon introduced impurities, is visible, although the C content is below $2{\cdot}10^{16}$ cm^{-3}. (For interpretation of the references to colour in this figure legend, the reader is referred to the web version of this article.)

unintentional oxygen incorporation in our MBE samples [30].

More specifically, YL was related to deep donor V_{Ga} transition in gallium lean n type GaN [21,31]. Armstrong et al. [13] claimed a deep level dependent of the concentration of C as dopant, which has a position in the band gap consistent with the YL. Furthermore, the YL centered around 2.2 eV was declared to be a phonon assisted transition from a shallow donor to an acceptor level [7]. For high carbon concentrations Armitage et al. [33] found that interstitial C related defects cause YL in C GaN by comparing the ionization energies for thermal quenching of the YL in SI C GaN and n type reference layers, while V_{Ga} is responsible for the YL at low C concentration [21,32]. However, ion implantation certainly creates other defects, such as V_{Ga}, which could result in the YL band, along with many other possibly known and un known defects [26]. Most of these defects are apparently not directly related to carbon [33].

Our approach is based on optimal MBE growth conditions to pre pare ultra pure hexagonal GaN with minimized defect density as a re ference along with similar material doped with an elemental solid state carbon source to avoid unintentional co doping effects, e.g. originating from organic precursors. The ultimate goal is to verify p type con ductivity in carbon doped hexagonal GaN. A prior step to electrical identification of the predicted p type conductivity in C doped GaN could be the spectroscopic identification of acceptor bound excitons, as e.g. reported in [34]. Surprisingly, our PL studies of carbon doped GaN at a level ~10^{18} cm^{-3} demonstrate that spectroscopic features hitherto associated with carbon or other acceptors are only weakly pronounced for the case of smooth surfaces arising from Ga rich growth conditions.

2. Materials and methods

In this study c axis, Ga polar and epitaxy ready 2″ **templates** and 1″ **substrates** were utilized as starting material for subsequent growth of wurtzite GaN layers. The templates were prepared by metal organic chemical vapor deposition (MOCVD) on sapphire and the free standing GaN was synthesized by hydride vapor phase epitaxy (HVPE). The thickness of the corresponding GaN layers ranges from 2 µm to 330 µm, resulting in defect densities between $5{\cdot}10^{9}$ cm^{-2} and $1{\cdot}10^{7}$ cm^{-2} for screw and mixed type dislocations [35,36]. The root mean square (RMS) roughness for all used templates and substrates was determined by AFM to be below 0.6 nm before the MBE overgrowth.

Growth was performed in a VG 80H plasma assisted MBE system (base pressure < 10^{-10} Torr). Prior to the MBE step all wafers and templates were out gassed in an ultra high vacuum environment (UHV) at above 500 °C for at least 4 h and transferred into the growth chamber under UHV conditions. Gallium with a purity of 8 N was evaporated from a single filament effusion source and active nitrogen (10 N) was supplied by an RF plasma source. Carbon is evaporated during growth from a pyrolytic graphite filament source (SUKO D type, MBE Komponenten GmbH, Germany; metal impurity level < 10 ppm, ac cording to vendor specification) and incorporated in the grown GaN

Provided by Sächsische Landesbibliothek - Staats- und Universitätsbibliothek Dresden

Final edited form was published in "Journal of Crystal Growth". 2019, 514, S. 29-35. ISSN 0022-0248.
https://doi.org/10.1016/j.jcrysgro.2019.02.041

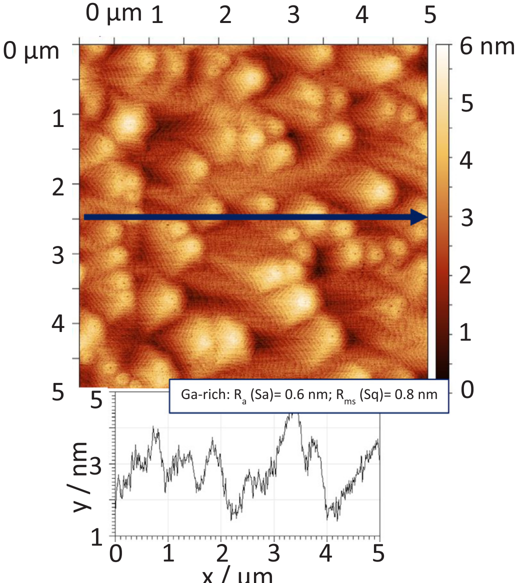

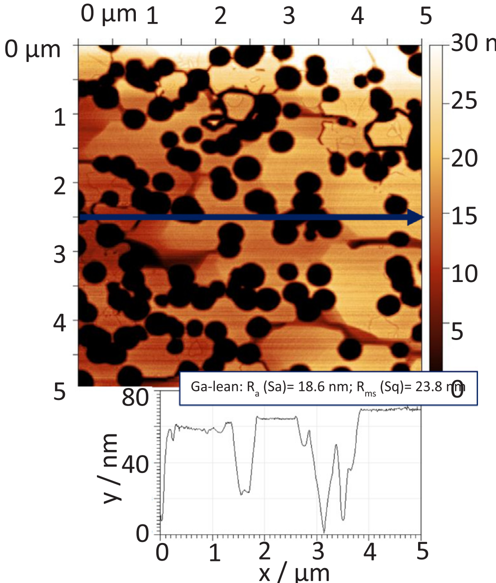

Fig. 4. AFM surface morphology from Ga-rich (left figure) and Ga-lean (right figure) regions of sample B showing monolayer steps and hillocks for the Ga-rich and monolayer steps with deep pits for the Ga-lean part of the sample. The according linescans and the overall surface roughness R_a and R_{ms} are presented below the respective AFM images.

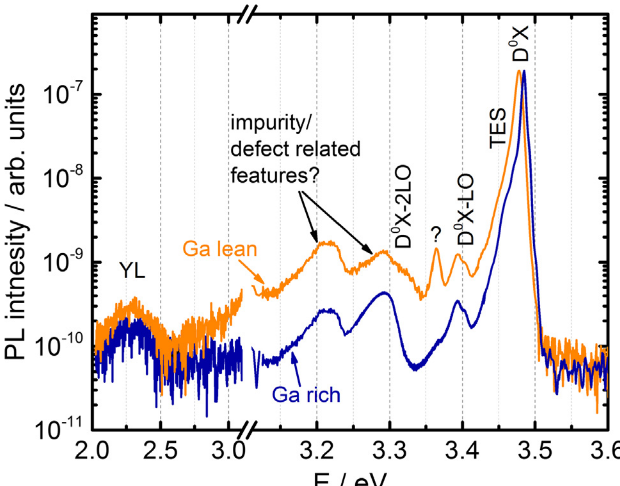

Fig. 5. PL spectra measured at 15K of a layered GaN sample (C) with C-doping levels of 10^{17} and 10^{18} cm^{-3}, prepared under Ga-lean growth conditions (orange) and under Ga-rich conditions (blue). Both regions exhibit the characteristic features assigned in literature to carbon impurities. In the Ga-lean region these features are more pronounced. Furthermore, the YL, which is normally associated with carbon introduced impurities, is visible at significantly reduced intensity compared to the other features.

films at a level of $1{\cdot}10^{18}$ cm^{-3} at a growth temperature of 650 °C. Undoped GaN samples are grown at a temperature of 700 °C, approximately 10 K below the rapid thermal desorption point for Ga on the wafer surface. At this higher growth temperature and identical operating conditions of the carbon source the incorporation drops to $1{\cdot}10^{17}$ cm^{-3}. The described procedure results in a growth rate of 240 nm/h and 2D growth mode of intrinsic material (for the undoped case) as reported elsewhere [30,37]. For the interpretation of the surface morphology data it is important to know that under the applied sample rotation the Ga/N ratio has a radial gradient of 2% from the wafer center towards the edge, which was extracted from thickness variations across the wafer. This inhomogeneity allows for Ga rich stoichiometry in the wafer center and Ga lean conditions towards the wafer edge in a single growth run.

The crystal surface morphology was monitored by atomic force microscopy (AFM) before and after MBE growth using a DI/Veeco DIMENSION 3100 AFM operated in contact mode.

The intentional and unintentional doping with O, C and Si was quantified by **secondary ion mass spectroscopy (SIMS)** in a Cameca ims 4f E6 system using Cs^+ at 14.5 keV, SI . For pre treatment the chamber was evacuated for at least 8 h and the samples were heated up in the UHV chamber for water desorption and outgassing. Implantation standards for ^{29}Si/GaN, ^{12}C/GaN and ^{16}O/GaN were measured in parallel for qualitative evaluation.

A central part in the **Photoluminescence (PL)** set up used here is a HeCd Laser with an excitation wavelength of 325 nm and an emitted power of 70 mW. The optical setup includes a bandpass filter to eliminate other laser lines, a chopper and optical components resulting in an excitation power of about 10 mW at the sample. A closed cycle cryostat allows for temperature dependent measurements between 400 and 15 K. The collected light was dispersed in a HORIBA Jobin Yvon THR1000 monochromator with a focal length of one meter and a 2400/mm grating for high spectral resolution. A Hamamatsu R928 photomultiplier tube was used as optical detector. All discussed spectra are scaled to the intensity maximum of the D^0X feature.

3. Results and discussion

Here we investigate PL features of carbon doped GaN grown by MBE to evaluate its potential acceptor character. The spectroscopic proof of the acceptor nature is a prerequisite towards demonstration of p type conductivity. Table 1 gives an overview of the four samples discussed including substrate specifications, preparation parameters and doping levels.

A 1 µm thick ultra pure MBE grown hexagonal GaN buffer of a 2DEG structure (sample A, see table 1) on a free standing, polished HVPE substrate with a remarkably low defect density between 10^7 (center) and 10^8 (edge) cm^{-2} serves as a clean reference system for PL investigations. The typical unintentional oxygen background, representing the only detectable impurity, was verified to be less than $1{\cdot}17$ cm^{-3} by SIMS. Such material is insulating at 300 K. In low temperature PL spectra (Fig. 1) the features exhibit narrow linewidth in both, the gallium lean and the gallium rich regions, typical for spectra shown in literature [39] thus manifesting the outstanding sample

Provided by Sächsische Landesbibliothek - Staats- und Universitätsbibliothek Dresden

Final edited form was published in "Journal of Crystal Growth". 2019, 514, S. 29-35. ISSN 0022-0248.
https://doi.org/10.1016/j.jcrysgro.2019.02.041

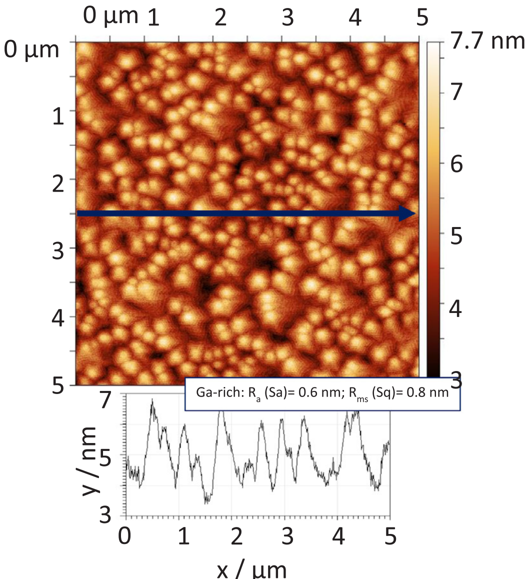

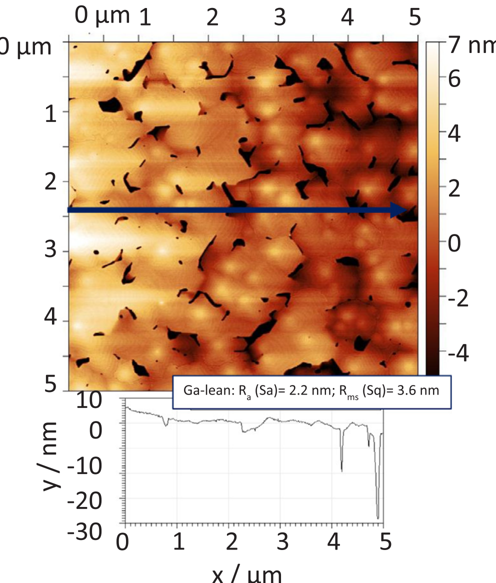

Fig. 6. AFM surface morphology from Ga-rich (left figure) and Ga-lean (right figure) region of sample C showing monolayer steps and hillocks for the Ga-rich and monolayer steps with deep pits for the Ga-lean region of the sample. The according linescans and the overall surface roughness R_a and R_{ms} are presented, below the respective AFM images.

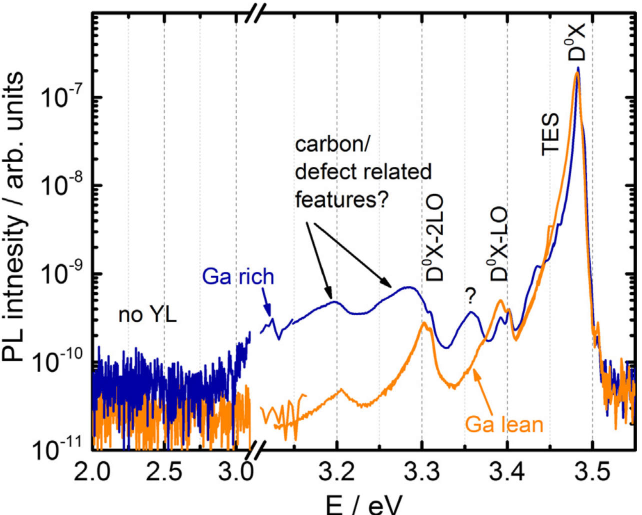

Fig. 7. PL spectra measured at 15K of a 400 nm thick C-doped GaN layer (sample D) with carbon content of 10^{18} cm^{-3} prepared under Ga-lean growth conditions (orange) and under Ga-rich conditions (blue). Both regions show more pronounced and broader features between 3.1 and 3.4 eV, as compared to the uid reference samples. The YL, which is normally associated with carbon introduced impurities, is not detectable. (For interpretation of the references to colour in this figure legend, the reader is referred to the web version of this article.)

quality. Donor bound exciton (D^0X) features are visible around 3.472 eV in a good agreement with literature [26]. At 3.480, 3.485 and 3.497 eV the A , B , and C transitions of free excitons are clearly iden tified. The multiple peak feature marked at 3.45 eV is assigned to two electron satellites (TES) transitions related to oxygen. The LO replicas of the main excitonic feature D^0X 1LO and D^0X 2LO can be found at 3.39 and 3.3 eV. The unidentified feature at about 3.36 eV found in several samples in this series and other samples grown in our laboratory will be addressed separately elsewhere. The difference between the two spectra plotted in Fig. 1 is the position on the wafer surface. The more intense spectroscopic features between 3.2 eV and the excitonic region are recorded at the edge area, exhibiting a higher defect density as identified in AFM surface morphology investigations (Fig. 2). This might be a first indication of defect related or enhanced occurrence of features in the PL spectra.

In the lower energy region at about 2.1 eV no yellow luminescence was detected which is a further indication of the relation between the residual oxygen level and the appearance of YL [37]. This sample re presents a reference with an unprecedented low residual impurity background and threading dislocation density. In the energy region down to 1.6 eV the second diffraction order of both, the excitonic fea tures at 1.73 eV as well as the laser line at 1.91 eV, can be found. Since no additional information can be extracted there, further PL spectra will be displayed in the energy range between 2.0 and 3.6 eV.

Sample B contains again a 1 µm thick uid MBE GaN layer but this time grown on a 2 µm MOVCD GaN template. It serves as a reference for the following intentionally doped samples C and D on similar sub strates. The PL data displayed in Fig. 3 resemble the basic spectroscopic features observed for sample A, but with broader linewidths of the observed peaks as compared to its counterpart on bulk GaN. Here, the defect and dislocation density was, as expected, higher which was confirmed by AFM surface scans as shown in Fig. 4. The defect density of the GaN layer is set by the defect density of the substrate [38]. PL features at 3.2 and 3.3 eV are historically assigned to dopants like Be, Mg, C, Si or O [26,39 45]. SIMS data for similar layers exclude these interpretations, since only oxygen is detectable and accounts to less than 10^{17} atoms /cm^3.

The obvious difference between the two PL scans in Fig. 3 is, again, the position on the wafer and, the different surface morphology as well as defect decoration as can be summarized from the AFM surface in vestigations in Fig. 4. In the Ga lean region with deep pits the char acteristic 'dopant' features are more pronounced. This is the second indication for defect related or enhanced occurrence of features in the PL spectra.

We now turn to sample C, which contains C and Si doped layers as described in Table 1 and was originally intended to serve as a cali bration sample for SIMS. The 60 nm thick C doped layer beneath the surface contains a carbon concentration of $1{\cdot}10^{18}$ cm^{-3} and will con tribute to carbon related features in PL spectra. Thus, the PL spectra in Fig. 5 show the same, but broadened and more intense peaks as the uid reference sample B (Fig. 3). Here, these dopant or impurity related features at 3.2 and 3.3 eV cannot be exclusively related to the dopant

Provided by Sächsische Landesbibliothek - Staats- und Universitätsbibliothek Dresden

Final edited form was published in "Journal of Crystal Growth". 2019, 514, S. 29-35. ISSN 0022-0248.
https://doi.org/10.1016/j.jcrysgro.2019.02.041

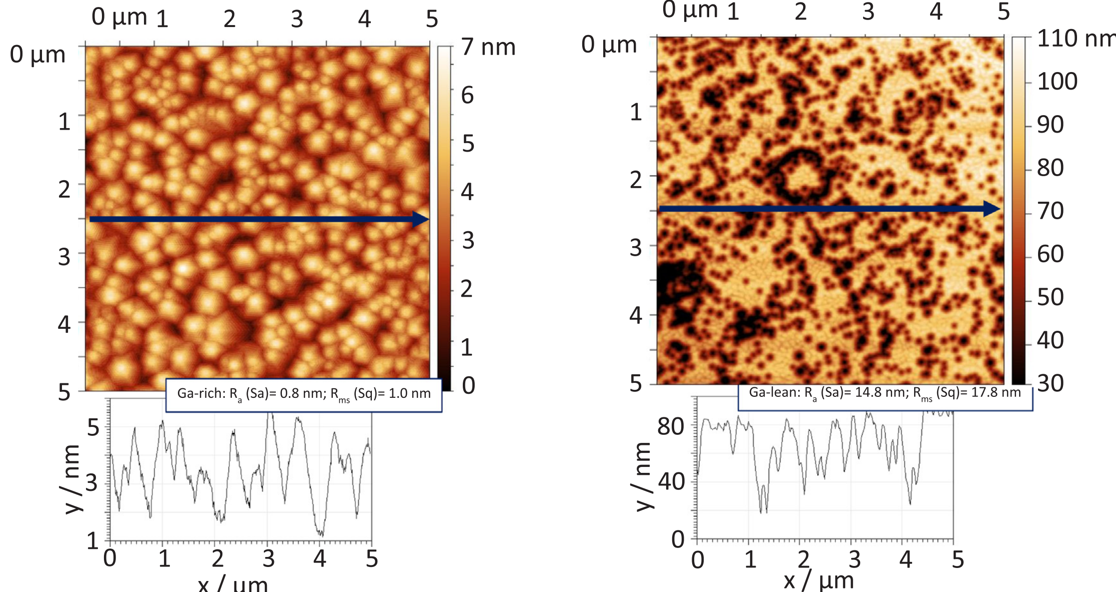

Fig. 8. AFM surface morphology from Ga-rich (left figure) and Ga-lean (right figure) region of sample D showing monolayer steps and hillocks for the Ga-rich and monolayer steps with deep pits for the Ga-lean region of the sample. The according linescans and the overall surface roughness R_a and R_{ms} are presented below the respective AFM image.

but more likely to the defect decoration caused by the substrate char acteristics. Yellow luminescence is detected around 2.2 eV but is not dominant compared to other features. In contrast to the undoped re ferences (sample A and B) or previously documented spectra [e.g. 10,32] the here documented YL is not markedly promoted.

Accompanying AFM investigations again prove the expected change of the surface morphology from the wafer center to the edge (Fig. 6). The Ga lean region shows the characteristic surface morphology with deep pits and occasional cracks as formerly described [40]. On the other side, the Ga rich layer features a smooth surface with monolayer steps and hillocks with 1 2 nm height. Here, AFM verifies a remarkable radial gradient of the defect decoration, which is caused by the sub strate and further more characteristic for a radial change in the Ga/N stoichiometry described before. The carbon content was found to be independent of the defect density, defect decoration and Ga/N stoi chiometry and was determined to be in the low 10^{18} atoms/cm^{-3} range by SIMS. This verifies the results by Green et al. [7] and Koblmüller et al. [12] and is in strong contrast to former reports where the carbon incorporation in GaN was found to depend on the Ga/N stoichiometry [19,43] (see Figs. 7and 8).

Sample D is a 400 nm thick C doped GaN layer grown on a 2 µm thick as grown MOCVD template with a carbon doping level of 10^{18} cm^{-3}. The PL data exhibit the above mentioned excitonic features D^0X around 3.472 eV and A /B /C transitions as well as TES and D^0X replicas in the energy range between 3.15 eV and 3.45 eV (Fig. 4). The Ga rich region shows an additional broad feature, at 3.28 eV over lapping the TES feature along with the feature at 3.19 eV. These were directly related to dopant impurities earlier [42,44 46]. Since they are found in the uid MBE layer (sample B), too, we cannot assign them exclusively to the C doping unlike the previous studies but to the defect decoration and density, caused by the variation in stoichiometry and by the template properties, respectively.

Contrary to the expectation, in the region of the YL the PL intensity is below the detection limit. Despite a carbon level of 10^{18} atoms/cm^3 and an elevated oxygen level (still below 10^{17} atoms/cm^3) in this sample the YL has practically vanished.

To conclude, under Ga lean and Ga rich growth conditions identical carbon levels evaporated from an elementary carbon source were incorporated, while the level itself depends on the sample temperature during MBE growth. Undoped reference layers as well as intentionally C doped GaN layers with a well known impurity background show the traditionally C related PL features at noticeable surface defect density. The results support that spectroscopic features between 3.0 and 3.3 eV are related to the surface morphology or defect landscape and do not originate exclusively from the carbon incorporation alone. Yellow lu minescence is widely absent in our carbon doped GaN (at level 10^{18} cm^{-3}) and oxygen lean (at level $\sim 2{\cdot}10^{16}$ cm^{-3}) reference samples and becomes pronounced for higher oxygen contents in elsewise un doped material. Under the growth conditions employed here, we con clusively exclude carbon as the origin of the yellow luminescence and suggest that its appearance is very likely related to the incorporated oxygen.

Acknowledgement

The TU Dresden part of the work was financially supported by the German Research Foundation (DFG) (project No. 348524434). The RAS part of the work was supported by the Russian Foundation for Basic Research (project No. 16 29 03168). The NaMLab gGmbH part of the work was financially supported by the German Federal Ministry for Economic Affairs and Energy BMWi (project No. 03ET1398B). The authors would like to thank RTG Mikroanalyse GmbH Berlin for SIMS measurements and discussion.

References

[1] S. Fischer, C. Wetzel, E.E. Haller, B.K. Meyer, Appl. Phys. Lett. 67 (9) (1995) 1298.
[2] P. Kozodoy, H. Xing, S.P. DenBaars, U.K. Mishra, J. Appl. Phys. 87 (4) (2000) 1832.
[3] Y.C. Chang, W.H. Chang, H.C. Chiu, L.T. Tung, C.H. Lee, K.H. Shiu, M. Hong, J. Kwo, J.M. Hong, C.C. Tsai, Appl. Phys. Lett. 93 (2008) 053504.
[4] G. Greco, F. Iucolano, F. Roccaforte, Appl. Surf. Sci. 383 (2016) 324–345.
[5] W. Götz, N.M. Johnson, J. Walker, D.P. Bour, H. Amano, I. Akasaki, Appl. Phys. Lett. 67 (18) (1995) 2666.
[6] W. Götz, N.M. Johnson, J. Walker, D.P. Bour, R.A. Street, Appl. Phys. Lett. 68 (5) (1996) 667.
[7] D.S. Green, U.K. Mishra, J.S. Speck, J. Appl. Phys. 95 (2004) 8456.
[8] C.H. Seager, A.F. Wright, J. Yu, W. Götz, J. Appl. Phys. 92 (2002) 6553.
[9] A.F. Wright, J. Appl. Phys. 92 (2002) 2575.
[10] H. Wang, A.-B. Chen, Phys. Rev. B 63 (2001) 125212.
[11] R. Armitage, Q. Yang, H. Feick, E.R. Weber, J. Cryst. Growth 263 (2004) 132–142.
[12] G. Koblmüller, R.M. Chu, A. Raman, U.K. Mishra, J.S. Speck, J. Appl. Phys. 107 (2010) 043527.

Provided by Sächsische Landesbibliothek - Staats- und Universitätsbibliothek Dresden

Final edited form was published in "Journal of Crystal Growth". 2019, 514, S. 29-35. ISSN 0022-0248.
https://doi.org/10.1016/j.jcrysgro.2019.02.041

[13] A. Armstrong, A.R. Arehart, D. Green, U.K. Mishra, J.S. Speck, S.A. Ringel, J. Appl. Phys. 98 (2005) 053704.
[14] C.R. Abernathy, J.D. MacKenzie, S.J. Pearton, W.S. Hobson, Appl. Phys. Lett. 66 (15) (1995) 1969.
[15] D.J. As, U. Kohler, J. Phys. Condens. Matter 13 (2001) 8923.
[16] S.J. Pearton, C.R. Abernathy, F. Ren, Electron. Lett. 30 (1994) 527.
[17] U. Birkle, M. Fehrer, V. Kirchner, S. Einfeldt, D. Hommel, S. Strauf, P. Michler, J. Gutowski, MRS Internet J. Nitride Semicond. Res. 4S1 (1999) G5.6.
[18] H. Tang, J.B. Webb, J.A. Bardwell, S. Raymond, J. Salzman, C. Uzan-Saguy, Appl. Phys. Lett. 78 (2001) 757.
[19] J.B. Webb, H. Tang, S. Rolfe, J.A. Bardwell, Appl. Phys. Lett. 75 (1999) 953.
[20] V. Fiorentini, L. F. Bernardini, A. Bosin, and D. Vanderbilt, Proceedings of the 23rd International Conference on Physics of Semiconductors (World Scientific, Singapore, 1996), Vol. 4, p. 2877.
[21] J. Neugebauer, C. Van de Walle, Appl. Phys. Lett. 69 (1996) 503.
[22] H.P. Maruska, J.J. Tietjen, Appl. Phys. Lett. 15 (1969) 327.
[23] P. Boguslawski, E.L. Briggs, J. Bernholc, Appl. Phys. Lett. 69 (1996) 233–235.
[24] A.Y. Polyakov, M. Shin, J.A. Freitas Jr., M. Skowronski, D.W. Greve, R.G. Wilson, J. Appl. Phys. 80 (1996) 6349.
[25] E.E. Reuter, R. Zhang, T.F. Kuech, S.G. Bishop, MRS Internet J. Nitride Semicond. Res. 4S1 (1999) G3.67.
[26] M.A. Reshchikov, H. Morkoç, J. Appl. Phys. 97 (2005) 061301.
[27] T. Suski, P. Perlin, H. Teisseyre, M. Leszczyński, I. Grzegory, J. Jun, M. Boćkowski, S. Porowski, T.D. Moustakas, Appl. Phys. Lett. 67 (1995) 2188.
[28] D.M. Hofmann, D. Kovalev, G. Steude, B.K. Meyer, A. Hoffmann, L. Eckey, R. Heitz, T. Detchprom, H. Amano, I. Akasaki, Phys. Rev. B Condens. Matter. 52 (23) (1995) 16702–16706.
[29] E. R. Glaser, T. A. Kennedy, J. A. Freitas, Jr., M. Asif Khan, D. T. Olsen, and J. N. Kuznia, Silicon Carbide and Related Materials, IOP Conf. Proc. No. 137 (IOP, Bristol, 1994), p. 443.
[30] S. Schmult, F. Schubert, S. Wirth, A. Großer, T. Mittmann, T. Mikolajick, J. Vac. Sci. Technol. B 35 (2) (2017) 02B104.
[31] E. Calleja, M.A. Sánchez-García, E. Monroy, F.J. Sanchez, E. Muñoz, A. Sanz-Hervas, C. Villar, M. Aguilar, J. Appl. Phys. 82 (1997) 4681.
[32] R. Armitage, William Hong, H. Qing Yang, J. Feick, E.R. Gebauer, S. Hautakangas Weber, K. Saarinen, Appl. Phys. Lett. 82 (2003) 3457.
[33] Z.-Q. Fang, D.C. Look, R. Armitage, Q. Yang, E.R. Weber, Mater. Res. Soc. Symp. Proc. 798 (2004) Y5.27.
[34] R. Stepniewski, A. Wysmołek, M. Potemski, K. Pakuła, J.M. Baranowski, I. Grzegory, S. Porowski, G. Martinez, P. Wyder, Phys. Rev. Lett. 91 (22) (2003) 226404.
[35] R.J. Molnar, W. Götz, L.T. Romano, N.M. Johnson, J. Cryst. Growth 178 (1997) 147.
[36] J.L. Weyher, S. Lazar, L. Macht, Z. Liliental-Weber, R.J. Molnar, S. Müller, V.G.M. Sivel, G. Nowak, I. Grzegory, J. Cryst. Growth 305 (2007) 384.
[37] F. Schubert, S. Wirth, F. Zimmermann, J. Heitmann, T. Mikolajick, S. Schmult, Sci. Technol. Adv. Mater. 17 (2016) 239.
[38] R. Hentschel, J. Gärtner, A. Wachowiak, A. Großer, T. Mikolajick, S. Schmult, J. Crystal Growth 500 (2018) 1–4.
[39] K. Kornitzer, T. Ebner, K. Thonke, R. Sauer, C. Kirchner, V. Schwegler, M. Kamp, M. Leszczynski, I. Grzegory, S. Porowski, J. Appl. Phys. 83 (1998) 4397.
[40] B. Monemar, P.P. Paskov, J.P. Bergman, A.A. Toropov, T.V. Shubina, S. Figge, T. Paskova, D. Hommel, A. Usui, M. Iwaya, S. Kamiyama, H. Amano, I. Akasaki, Mater. Sci. Semicond. Process. 9 (2006) 168–174.
[41] B. Monemar, et al., Jpn. J. Appl. Phys. 5208JJ03 (2013).
[42] A.J. Ptak, et al., Mater. Res. Soc. Sypm. Proc. 639 (2001) G3.3.
[43] D.J. As, D.G. Pacheco-Salazar, S. Potthast, K. Lischka, Mat. Res. Soc. Symp. Proc. 798 (2004).
[44] J.E. Northrup, Phys. Rev. B 66 (2002) 045204.
[45] J. Elsner, R. Jones, M.I. Heggie, P.K. Sitch, M. Haugk, Th. Frauenheim, S. Öberg, P.R. Briddon, Phys. Rev. B 58 (1998) 12571.
[46] L.W. Tu, Y.C. Lee, D. Stocker, E.F. Schubert, Phys. Rev. B 58 (1998) 10696.

Provided by Sächsische Landesbibliothek - Staats- und Universitätsbibliothek Dresden